International Journal of Biological Macromolecules 89 (2016) 238–245

Contents lists available at ScienceDirect

International Journal of Biological Macromolecules

journal homepage: www.elsevier.com/locate/ijbiomac

Multimeric species in equilibrium in detergent-solubilized Na,K-ATPase

Juliana Sakamoto Yoneda[a,b,1], Gustavo Scanavachi[a,1], Heitor Gobbi Sebinelli[b], Júlio Cesar Borges[c], Leandro R.S. Barbosa[a], Pietro Ciancaglini[b], Rosangela Itri[a,*]

[a] Instituto de Física da Universidade de São Paulo, IF USP, 05508-090 São Paulo, Brazil
[b] Faculdade de Filosofia Ciências e Letras de Ribeirão Preto, FFCLRP USP, 14040-901 Ribeirão Preto, SP, Brazil
[c] Instituto de Química de São Carlos, IQSC-USP, 13560-970 São Carlos, SP, Brazil

ARTICLE INFO

Article history:
Received 9 January 2016
Received in revised form 19 April 2016
Accepted 20 April 2016
Available online 21 April 2016

Keywords:
Na-K,ATPase
Oligomerization
Equilibrium state

ABSTRACT

In this work, we find an equilibrium between different Na,K-ATPase (NKA) oligomeric species solubilized in a non-ionic detergent $C_{12}E_8$ by means of Dynamic Light Scattering (DLS), Analytical Ultracentrifugation (AUC), Small Angle X-ray Scattering (SAXS), Spectrophotometry (absorption at 280/350 nm) and enzymatic activity assay. The NKA sample after chromatography purification presented seven different populations as identified by AUC, with monomers and tetramers amounting to ~55% of the total protein mass in solution. These two species constituted less than 40% of the total protein mass after increasing the NKA concentration. Removal of higher-order oligomer/aggregate species from the NKA solution using 220 nm-pore filter resulted in an increase of the specific enzymatic activity. Nevertheless, the enzyme forms new large aggregates over an elapsed time of 20 h. The results thus point out that $C_{12}E_8$-solubilized NKA is in a dynamic equilibrium of monomers, tetramers and high-order oligomers/subunit aggregates. These latter have low or null activity. High amount of detergent leads to the dissociation of NKA into smaller aggregates with no enzymatic activity.

1. Introduction

Na,K-ATPase (NKA) is a member of the P-type family of active cation transport proteins present in the plasma membrane of all mammalian cells. It is usually purified from different NKA-rich tissues from kidney and brain, for instance [1–4], and consists of two main polypeptide chains: the α (~110 kDa) and β-subunits (~35–50 kDa) [5,6]. The α-subunit possesses the cation-binding sites, and undergoes conformational changes during the active transport. The β-subunit, on the other hand, is required for translation, stability, and membrane insertion of NKA. Furthermore, this subunit can self-associate, giving a cell–cell adhesion function to the enzyme [7]. A third, small (~7–12 kDa) and hydrophobic subunit (γ-subunit in the kidney) can also be found in the NKA [8].

NKA uses ATP hydrolysis to transport three Na^+ ions out of the cell, whereas it pumps two K^+ ions into the cell, against their concentration gradients [9]. The Na^+ gradient generated drives many transport processes through co-transporters (sodium glucose), exchangers (Na^+/Ca^{2+}) and also drives amino acids and vitamin transport into the cells [9]. Besides, the electrochemical gradient is essential for physiological processes such as electrical excitability, nerve transmission, and muscle contraction [10,11]. The transport of Na^+ and K^+ is accomplished by the enzyme conformational changes [12]. In general, two main conformational states exist: the sodium-bound E1 state and the potassium-bound E2 state, which were well elucidated by the corresponding crystallographic structures [13,14].

Although NKA is well known since its first description in 1957 [15], the functional unit of the enzyme is still a matter of debate. The main issue concerns whether the enzyme native state in cell membranes is a αβ-monomer or $(\alpha\beta)_n$ oligomers [16]. It has been previously reported that the monomer is capable to transport ions [17]. Therefore, there is no structural reason for ion pumps to aggregate into dimers or higher oligomers in order to translocate ions. Nevertheless, several authors have suggested the involvement of diprotomers or higher oligomers in the mechanism of the Na,K-ATPase in native membranes [18]. A comparison of the extent of phosphorylation with ligand-binding capacities in the presence and absence of ATP hydrolysis strongly suggests that the functional unit of NKA in the membrane is a tetramer, $(\alpha\beta)_4$ [16]. Besides,

* Corresponding author.
E-mail addresses: itri@if.usp.br, rosangela.itri@gmail.com (R. Itri).
[1] These authors contributed equally to this paper.

http://dx.doi.org/10.1016/j.ijbiomac.2016.04.058
0141-8130/

there are evidences for associations among monomers as revealed by cross-linking experiments, single particle imaging and thermal inactivation studies [17,19–22]. Thus, the self-association of Na,K-ATPase could play a crucial role in biological system, however the functional importance of multimeric interactions between the active pump enzymes remains unproven [4,23].

It is well known that the methods employed for solubilization and purification of NKA may influence the aggregation of the enzyme and the stoichiometry of the ($\alpha\beta$) protomers [24,25]. In studies with membrane proteins, the use of detergent is essential to keep the protein of interest in the functional state out of the bilayer [26]. Integral proteins solubilized with non-ionic detergents can retain their native structure and activity for a considerable time. The detergent/protein ratio is a critical parameter for aggregation and/or denaturation after removal from the hydrophobic medium of the lipid membrane [27].

In particular, our group investigated how the surfactant:protein, $C_{12}E_8$:NKA molar ratios influence the enzyme solubility and its reconstitution in proteoliposomes by different biophysical techniques [28–32]. Circular dichroism, surface tension and dilatational elasticity revealed changes in the enzyme secondary structure, whereas DSC measurements evidenced $C_{12}E_8$ concentration dependent differences in thermal stability of $C_{12}E_8$-solubilized NKA, in the low concentration range [28–33]. At high $C_{12}E_8$ concentrations, the enzyme dissociation, followed by self-assembling of α-subunit into α_4 aggregates was determined by means of Small Angle X-ray Scattering (SAXS) measurements [34]. It should be stressed, however, that different NKA concentrations ranging from 0.01 to 5 mg mL^{-1} were used, depending on the method employed. Noteworthy, NKA enzymatic activity is usually evaluated at protein concentrations in the order of 10^{-3} mg mL^{-1} [29,30].

In previous reports [29,30], the NKA species present in solution right after solubilization in $C_{12}E_8$ and purification were not addressed. In the present work, NKA solubilized using 1 mg of $C_{12}E_8$ to 1 mg of protein, the condition for maximum solubilization and activity [35], is revisited with the aim of identifying the main multimeric species in solution and how these can change under the action of external factors. In fact, we here demonstrate that the monomer ($\alpha\beta$) coexists with oligomeric forms and non-functional aggregates (or with low enzymatic activity), even after the gel filtration. Different approaches were used to avoid and to remove higher-order aggregates from freshly prepared NKA samples. Noteworthy, most of the reported studies on NKA were performed assuming that the protein was in a single oligomeric state [24,36,37], which is not generally true for all NKA purification procedures. Our results thus emphasize the importance of the knowledge of the oligomeric forms present in NKA samples in order to avoid misleading data interpretations.

2. Materials and methods

2.1. Material

All samples were prepared using Millipore Direct-Q ultrapure apyrogenic water, and all reagents were of the highest purity commercially available: Trichloric Acetic Acid (TCA); tris[hydroxymethyl]aminomethane (Tris); *N*-(2-hydroxyethyl) piperazine-*N*′-ethanesulfonic acid (HEPES); ATP; BSA and Dodecyloctaethyleneglycol ($C_{12}E_8$) were from Sigma; SDS was from Lancaster. EDTA, potassium chloride, sodium chloride and magnesium chloride were from Merck. Biobeads were from BioRad. Sterile filters of 220 nm and 100 nm pores were purchased from Millipore.

2.2. $C_{12}E_8$-Na,K-ATPase preparation

Solubilized and purified NKA (E.C 3.6.3.9) was extracted from the dark red outer medulla of the kidney of adult New Zealand white rabbits as previously described [35]. Briefly, the kidney tissue was homogenized in a high-speed shearing homogenizer and ultracentrifuged. The pellet corresponding to membrane-bound NKA was resuspended. One milligram of NKA membrane fragments with 1 mg of $C_{12}E_8$ were mixed at 4 °C. After ultracentrifugation, the supernatant was assayed for protein concentration and ATPase activity. The $C_{12}E_8$-solubilized enzyme was purified by gel filtration at 4 °C on a Sepharose 6B column (1.4 × 119 cm) and fractions showing ATPase activity were pooled. Samples were concentrated through a YM-10 Amicon filter when necessary.

Protein concentration was estimated in the presence of 2% (w/v) SDS as described in Ref. [35]. BSA was used as standard.

2.3. ATPase activity

ATPase activity (V_{max}) was assayed discontinuously at 37 °C using a spectrophotometer Spectronic Genesis 2 (Milton Roy) by quantification of the phosphate release, in a buffer composed by HEPES 50 mmol L^{-1} at pH 7.5 in the presence of saturating concentration of ATP (3 mmol L^{-1}), KCl (10 mmol L^{-1}), $MgCl_2$ (5 mmol L^{-1}) and NaCl (50 mmol L^{-1}), in a final volume of 1.0 mL, as reported in Ref. [35]. The reaction was initiated by addition of the enzyme, and stopped by 0.5 mL of cold 30% TCA as previously described in Ref. [35]. The tubes were then kept in ice and immediately centrifuged for 10 min. The amount of inorganic phosphate produced by ATP hydrolysis was measured using the method described by Heinonen and Lahti [38].

Assays were performed in triplicate and controls without added enzyme were included in each experiment to quantify the non-enzymatic hydrolysis of the substrate. The reactions were started by addition of enzyme or substrate depending of the system used. Specific activity (enzyme unit—U) is defined as the amount of enzyme hydrolyzing 1.0 nmol of ATP per minute at 37 °C per mg of protein.

2.4. Dynamic light scattering

Size distribution of solubilized protein was determined using a N5 Submicron Particle Size Analyzer (Beckman Coulter, Inc., Fullerton, CA, USA). A 25 mW Helium-Neon laser was used as the light source with wavelength $\lambda = 632.8$ nm, at a scattering angle of 90°. The results presented here are the average of five measurements, and the weighted average (WA) of the hydrodynamic radii was determined as $WA = \Sigma\ r_i w_i$ where r_i is the hydrodynamic radius and w_i is the weight [39] corresponding to i distributions. Assays were performed in triplicate using different enzyme preparations.

2.5. Analytical ultracentrifugation

The protein solubilized and purified according to Section 2.2 was subjected to sedimentation-velocity-analytical-ultracentrifugation (SV-AUC) experiments in a Beckman Optima XL-A analytical ultracentrifuge using the AN50-TI rotor. The protein was centrifuged at 12,000 rpm (13 °C) in different concentrations before and after filtration through a 100 nm-pore filter. The sedimentation rate was recorded at 227 nm. Both non-concentrated (~0.1 mg mL^{-1}) and concentrated (~0.4 mg mL^{-1}) samples were also subjected to SV-AUC at 18000 RPM (13 °C) and data collection was at 236 nm. The sedimentation rate data was analyzed by SedFit software, version 14.1 [40] in order to obtain the c(S) curves. The apparent sedimentation coefficients (s) were obtained from the maxima of the peaks of c(S) distribution

curves and corrected for standard conditions ($s_{20,w}$) of water at 20 °C [41], using the Sednterp software (http://sednterp.unh.edu/). This software was also used for estimating buffer viscosity ($\eta = 1.0045 \times 10^{-2}$ poise), density ($\rho = 1.00055\ g\ mL^{-1}$) and protein partial-specific volume ($V_{bar} = 0.7412\ mL\ g^{-1}$). The relative amount of each species, observed in the SV-AUC experiments, was determined by taking into account the area under each peak in the c(S) curve.

The crystallographic structures for NKA (PDB Acc. numbers 3WGV and 3A3Y) as "monomer" ($\alpha\beta$) and "dimer unit" $(\alpha\beta)_2$ were analyzed by the HydroPro software [42] in order to obtain their hydrodynamic and structural properties, allowing comparison with the one's determined experimentally. The hydrodynamic parameters were determined for standard conditions.

2.6. Absorption spectroscopy

The UV–vis spectra were measured in an Ultrospec 5300 Pro spectrophotometer from Amersham Biosciences (Amersham Biosciences, Corp., NJ, USA), using quartz cells with 1 cm path-length. Each spectrum was recorded from 200 to 450 nm with scan step and scan speed of 1 nm and 1856 nm/min, respectively.

The absorption bands of proteins (without metallic groups) range from approximately 200–300 nm. In particular, tryptophan absorbs at $\lambda = 280$ nm enabling protein concentration determination at this wavelength [43,44]. On the other hand, when large oligomers and aggregates are present, the solution turns turbid, causing scattering of light for $\lambda > 330$ nm [45,46]. In this way, protein oligomerization and aggregation were evaluated by observing the changes in absorption value at 280 nm, as well as the turbidity value at 350 nm over time.

2.7. Small angle X-ray scattering

The experiments were performed at the National Synchrotron Light Laboratory (LNLS-SAXS1 beamline, Campinas, Brazil), radiation wavelength $\lambda = 1.488$ Å, sample-to-detector distance of ~1300 mm, and at room temperature of 25 °C. Samples were filtered through 100 nm-pore filters and set between two mica windows with a 1 mm spacer. The sample holder was placed perpendicular to the incident X-ray beam. The obtained curves (data collection of 5 min) were normalized by taking into account the decrease of the X-ray beam intensity during the experiment. The parasitic background from the buffer solution was subtracted considering the sample's attenuation. Purified NKA samples were prepared in the absence and presence of 0.5 and 1 mM SDS.

The scattering intensity, I(q), of an isotropic solution of non-interacting scattering particles can be described as [47] $I(q) = kn_p P(q)$, where k is an experimental factor and n_p the particle number density, q is the modulus of the scattering vector, $q = 4\pi\ sin(\theta)/\lambda$, 2θ being the scattering angle, and P(q) is the form-factor.

It is possible to calculate the protein form-factor directly from the crystallographic structure. In the present work, we made use of the SASMOL software [48] to calculate P(q) of both monomer ($\alpha\beta$) and dimer $(\alpha\beta)_2$ structures (PDB entry: 3WGV, [14]).

In the absence of interference effects, a Fourier transform connects the scattering intensity I(q) to the pair distance distribution function, p(r), which provides information about the protein size, shape, radius of gyration, R_g, as well as its maximum dimension, D_{max}, [47,49,50]. In this work, the GIFT software [51] was employed to obtain the p(r) functions from the whole set of SAXS curves.

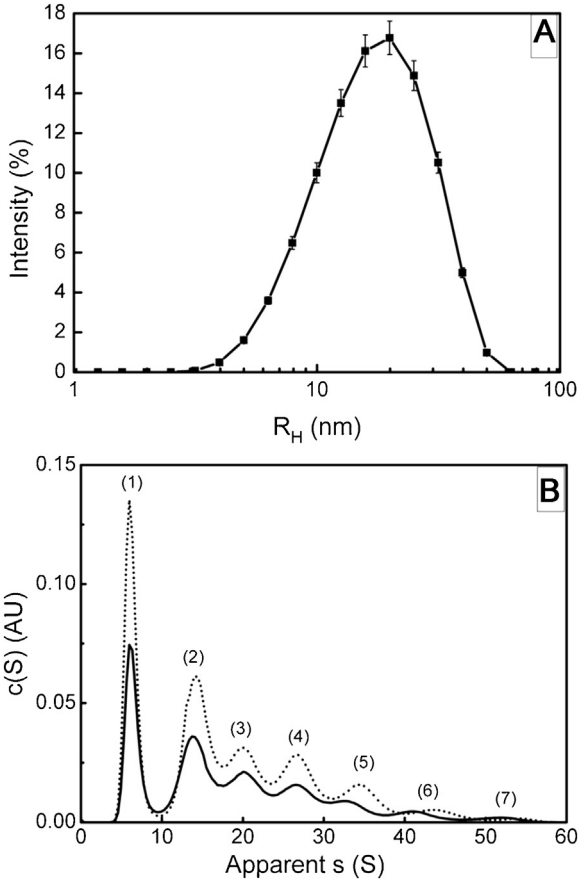

Fig. 1. (A) Distribution of Hydrodynamic Radius, R_H, evaluated by DLS of $C_{12}E_8$-solubilized NKA after chromatography. Protein concentration was 0.07 mg mL^{-1}. (B) c(S) curves for non-concentrated NKA samples after filtration (---) 0.06 mg mL^{-1}, (·····) 0.10 mg mL^{-1}. The SV-AUC experiment was done at 12,000 rpm and 13 °C. A total of 200 absorbance scans over the cell radius were collected at 227 nm and treated by SedFit software (version 14.1).

3. Results and discussion

3.1. $C_{12}E_8$ solubilized-NKA characterization: DLS and AUC measurements after purification

Fig. 1A shows the DLS results obtained from solubilized NKA samples (0.07 mg mL^{-1}) immediately after elution from the purification column. The sample was eluted with a buffer containing 0.005 mg mL^{-1} of $C_{12}E_8$. An inspection of the data reveals that the sample is composed of different species, with a size distribution centered at the weighted average of 19 ± 1 nm. The expected Stokes Radius (R_s) values for ($\alpha\beta$) and $(\alpha\beta)_2$ are 5.0 nm and 6.3 nm, respectively, calculated from the NKA crystallographic structure for the monomer (PDB: 3WGV and 3A3Y) and the dimer (PDB: 3WGV) (Table 1). Therefore, DLS results evidenced that the eluted enzyme may contain several $(\alpha\beta)_n$ oligomer species. Moreover, the possibility of other types of self-assembled subunit aggregates like $(\alpha)_n$, $(\beta)_n$ or $(\alpha_n\beta_m)$ cannot be disregarded. It should be noted that the PDB files include the γ subunit, although our samples lack this because of the solubilization process employed [31]. However, the contribution from this subunit is negligible for DLS results due to its smaller size as compared to α- and β-subunits.

We continue the investigation using AUC measurements to pursue which oligomeric species were present in NKA solutions of 0.06 mg mL^{-1} and 0.10 mg mL^{-1}. For this, the sample was first filtered through 100 nm-pore to ensure a selection of the species below this dimension. The filtered NKA samples showed that there

Table 1
Structural and hydrodynamic properties predicted from NKA crystallographic structure for a monomer (PDB: 3WGV and 3A3Y) and dimer (PDB: 3WGV) by HydroPro software. Molecular Mass (MW) determined from their amino acid sequence, Stokes Radius (R_s), Radius of gyration (R_g), Sedimentation coefficient at standard conditions ($s_{20,w}$), Maximum Sedimentation coefficient (s_{max}), and Maximum distance (D_{max}), Frictional ratio (f/f_0).

PDB	$(\alpha\beta\gamma)_n$	MW (Da)	R_s (nm)	R_g (nm)	$s_{20,w}$ (S)	s_{max} (S)[a]	D_{max} (nm)	f/f_0[b]
3A3Y	1	156499	5.0 ± 0.1	4.7 ± 0.1	7.1 ± 0.1	9.9	17.1	1.4
3WGV	1	154490	5.1 ± 0.1	4.7 ± 0.1	7.0 ± 0.1	9.8	16.7	1.4
3WGV	2	308980	6.3 ± 0.1	5.4 ± 0.1	11.2 ± 0.1	15.6	18.3	1.4

[a] Theoretical s-value predicted for a spherical particle of a give MW.
[b] Estimated by the ratio of s_{max} and the predicted $s_{20,w}$-value for each crystallographic structure.

is a high degree of size polydispersity in both protein concentrations tested (Fig. 1B). Table 2 summarizes the properties and the relative amount of each species according to the AUC data analysis. At least 7 species in solution were identified. It should be stressed, however, that the first two species (Table 2) amounts for ~55% of the protein mass in solution.

According to Table 1, considering the hydrodynamic parameters evaluated from the crystallographic structures, we can conclude that species (1) might be attributed to NKA monomer ($\alpha\beta$). The predicted $s_{20,w}$-value for ($\alpha\beta$) was of about 7 S in a good agreement with the experimental value of 7.2–7.4 S and it corresponds to a MW of ~180 kDa. The specie (2) presented a $s_{20,w}$-value of about 17 S, which was higher than that predicted for $(\alpha\beta)_2$ (Table 1) and also higher than for a spherical protein of around 300 kDa. The maximum s-value (s_{max}) estimated for a globular protein of 300 kDa is around 15.6 S (determined by Sednterp software), indicating that the specie (2) should be an oligomer larger than $(\alpha\beta)_2$. It is probably a tetramer, since the molecular mass obtained experimentally (Table 1) is approximately 4 times the MW for the monomer as estimated by the SedFit software (Table 2). Furthermore, it is also possible to observe five other populations of higher molecular mass, suggesting the presence of larger oligomers $(\alpha\beta)_n$ and/or sub-units aggregates (Fig. 1B). However, the results have no resolution to attribute the stoichiometry of these species, mainly considering the absence of other structural information.

Interestingly, the frictional ratio (f/f_0), which is a shape factor obtained from hydrodynamic techniques, estimated by the ratio of s_{max} and the experimental $s_{20,w}$ calculated for the species (1) and (2) considered as monomer and tetramer amounted to ~1.3 and 1.4, respectively. These f/f_0-values thus indicate that the NKA species (1) and (2) have a slightly elongated shape as do the crystallographic structures (Table 1).

In agreement with DLS data, AUC results show that after purification $C_{12}E_8$-solubilized NKA (1 mg protein: 1 mg $C_{12}E_8$) presents different oligomeric species in solution, that is, monomers, tetramers, higher-order oligomers and/or aggregates. Previously reported protocols in the literature suggested that $C_{12}E_8$-solubilized NKA can be found in a variety of oligomeric species: monomer [36,37,52–55], dimer [24,55,56], trimer [54] and tetramer [19,57]. Therefore, the discrepancies found between our results and those reported in the literature can be probably attributed to different conditions used in the solubilization process. As remarked before, the type of surfactant and the detergent/protein ratio are the key factors that may drive the self-association of protomers $(\alpha\beta)_n$ and/or subunits of the solubilized NKA.

3.2. The effect of NKA concentration: DLS and AUC measurements

In order to investigate how NKA concentration impacts on the association of the multimeric species, freshly prepared samples were concentrated through a YM-10 Amicon filter. Such procedure induced the formation of aggregates larger than those found in non-concentrated NKA samples, as evidenced by the appearance of scatters with hydrodynamic radii >100 nm (Fig. 2A). To identify which oligomeric states were presented in the filtered and concentrated samples, SV-AUC experiments were also employed (Fig. 2B). As one can see in Fig. 2B, there are at least 14 different species in solution at 0.4 mg mL^{-1}. AUC data analysis indicated that the five main species observed in the non-concentrated samples (species (1)–(5), Fig. 1B) account for 95% of the protein mass, decreasing to 60% at 0.4 mg mL^{-1}. Interestingly, the species (1) and (2) present in the concentrated sample constituted less than 40% of the protein mass in solution, whereas they amounted to 55% in the non-concentrated samples (Table 2). Thus, concentration indeed induces formation of higher-order oligomers or subunit aggregates.

Therefore, the combined DLS and AUC results give support to the conclusion that $C_{12}E_8$-solubilized NKA in solution is an equilibrium of different oligomeric states (even after elution).

In order to better understand the equilibrium of NKA species over time and how this impact the enzymatic activity assays, a series of experiments were realized as follows.

3.3. Filtering the concentrated NKA

In order to remove the larger species from concentrated samples, filters of 220 nm-pore size were used. Fig. 3 displays the absorption spectra from concentrated samples, and right after filtration. As one can see, there is a 26% reduction in the absorbance value at 280 nm, indicating a decrease in the protein concentration. Moreover, there is a reduction of 57% in the turbidity value at

Table 2
Hydrodynamic parameters obtained for each NKA species from SV-AUC experiments.

Species	NKA 0.06 mg mL^{-1}			NKA 0.1 mg mL^{-1}		
	$s_{20,w}$ (S)[a,b]	MW (kDa)[a]	Amount (%)	$s_{20,w}$ (S)[a]	MW (kDa)[a]	Amount (%)
1	7.4	190	26	7.2	180	26
2	16.4	620	29	17.7	620	28
3	23.5	1080	18	23.6	1050	17
4	31.3	1640	16	31.2	1590	16
5	38.9	2280	7	40.2	2320	10
6	48.0	3110	5	51.1	3330	4
7	59.3	4280	2	62.0	4460	1

[a] Errors are of 5%.
[b] Values of apparents (from Fig. 2B) normalized to standard conditions of water and 20 °C.

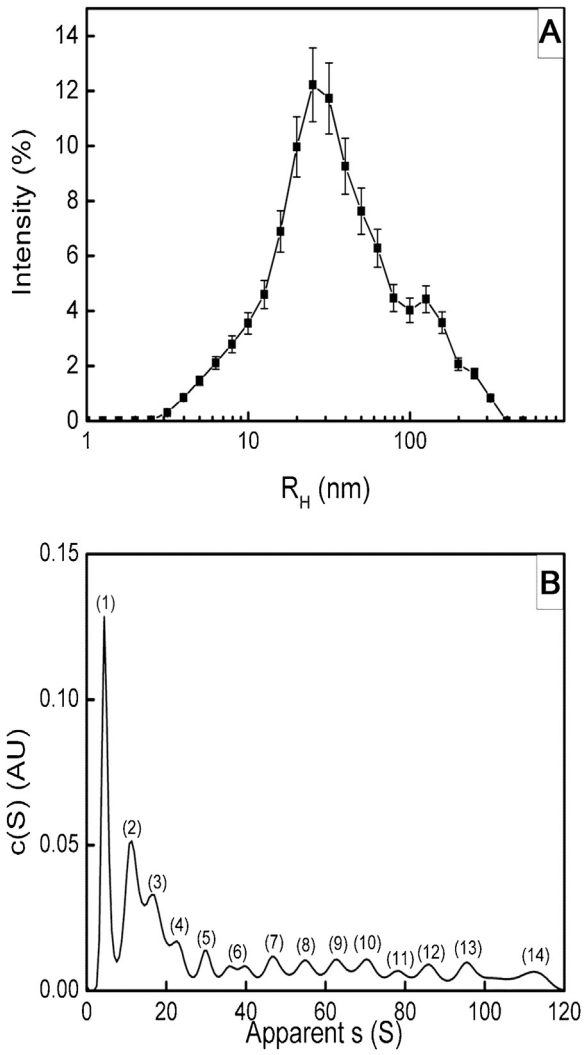

Fig. 2. (A) Distribution of Hydrodynamic Radius, R_H, evaluated by DLS of $C_{12}E_8$-solubilized NKA after passing through a YM-10 Amicon filter resulting in an enzyme concentration of 0.68 mg mL^{-1}. (B) c(S) curves for concentrated NKA samples after filtration (0.4 mg mL^{-1}). The SV-AUC experiment was performed at 18,000 rpm and 13 °C. A total of 100 absorbance scans over the cell radius were collected at 236 nm and treated by SedFit software (version 14.1).

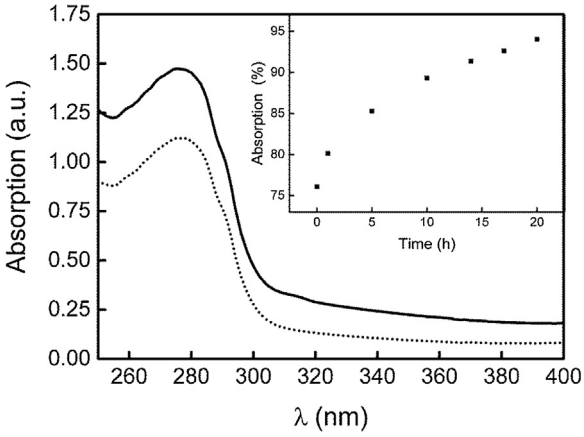

Fig. 3. Absorption spectrum of NKA before (---) and after (·····) filtration with 220 nm-pore size. *Inset*: Absorption at 280 nm of NKA after filtration with 220 nm-pore as a function of time. The intensity was normalized by the absorption of the sample before filtration.

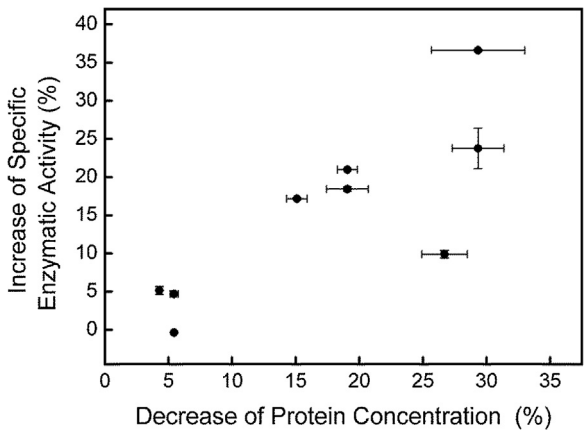

Fig. 4. Increase of specific enzymatic activity as a function of decrease in NKA concentration after filtration with 220 nm-pore. Each point is the result of specific enzymatic activity and protein concentration measurement of the same sample before and after filtration, considering 100% specific enzymatic activity and protein concentration before filtration.

350 nm, implying filtration indeed removes large species (>220 nm) in the sample.

The decrease in size after filtration is confirmed by a reduction of 42% in the WA value (Fig. S1—Supplementary material), which indicates that some higher-order oligomers and large aggregates were excluded from the sample. However, DLS measurements still exhibit a distribution in size, indicating the existence of populations with different molecular masses (Fig. S1).

In order to verify if the NKA species evolve with time, absorption measurements at 280 nm were performed after filtration. As shown in Fig. 3 (inset) the normalized absorption at 280 nm increases while the protein concentration is kept constant. It means that the increase in absorption must be caused by an increase in light scattering due to the formation of larger aggregates in solution [58]. Furthermore, the scattering intensity 20 h after filtration, amounted to 96% (normalized), which indicates that the higher oligomers and/or aggregates must have formed as those observed prior to filtration.

Also, populations larger than 220 nm in size arise with time, indicating an increase of size polydispersity (Fig. S2A) and the weighted average (WA) over time, as one can see in Fig. S2B.

Interestingly, Fig. 4 presents the variation of specific enzymatic activity and protein concentration of the same sample before and right after filtration. As one can verify, the filter reduces the protein concentration to ~30% and this is accompanied by an increase of specific enzymatic activity (up to 37%). Therefore, populations larger than 220 nm (pore size) show a tiny or no enzymatic activity, since its removal leads to a similar enzymatic activity as before filtration. The enzymatic activity after the removal of larger aggregates must be due to the presence of some NKA oligomeric forms. Actually, it is well known in the literature that different subunits associations, catalytically competent, can exist in solution as monomer $(\alpha\beta)$ [58,59], dimer $(\alpha\beta)_2$ [58–60], trimer $(\alpha\beta)_3$, and/or tetramer $(\alpha\beta)_4$ [16,33,59,61]. Of note, associations of β in higher orders were reported in the sample of NKA solubilized in SDS and tris dodecyl sulfate (TDS) or in membrane fraction [62,63]. Also, associations of α in higher orders [62,64] can be found as α_4 [34]. However, the oligomeric species consisted by α_n or β_m have no enzymatic activity [12].

Therefore, filtration retains populations larger than 220 nm. Nevertheless, the remaining populations in solution do self-assemble towards new oligomers and/or aggregates with time. These results suggest that the equilibrium of NKA solubilized and purified in $C_{12}E_8$ is reached in the presence of different

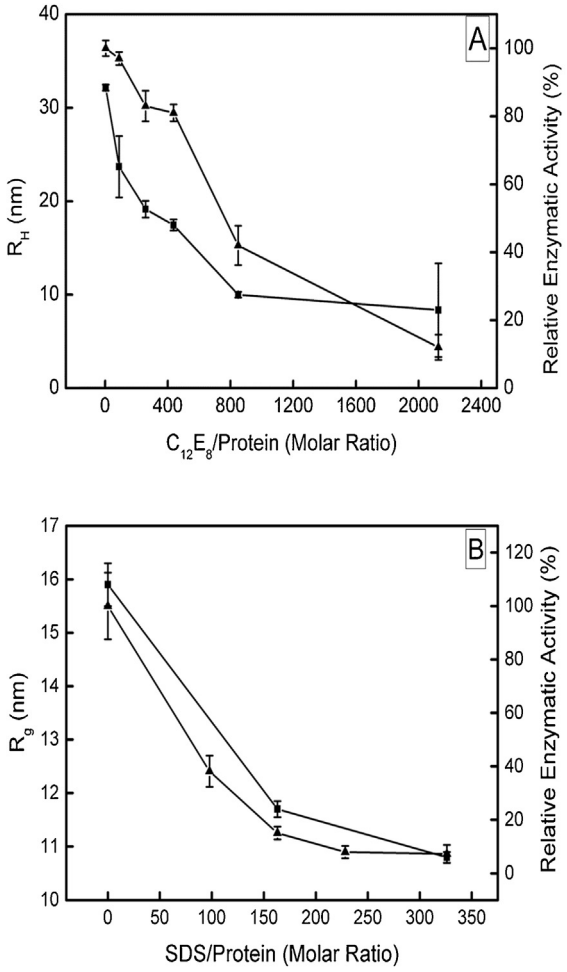

Fig. 5. (A) Hydrodynamic Radius (R_H) (■) and Relative Enzymatic Activity (▲) of solubilized NKA with increase in $C_{12}E_8$/Protein. Protein concentration was 0.37 mg mL^{-1}. All values are the average ± SD for three determinations. (B) Radius of Gyration (R_g) (■) and Relative Enzymatic Activity (▲) of solubilized NKA with increase in SDS/Protein. Protein concentration was 0.46 mg mL^{-1}.

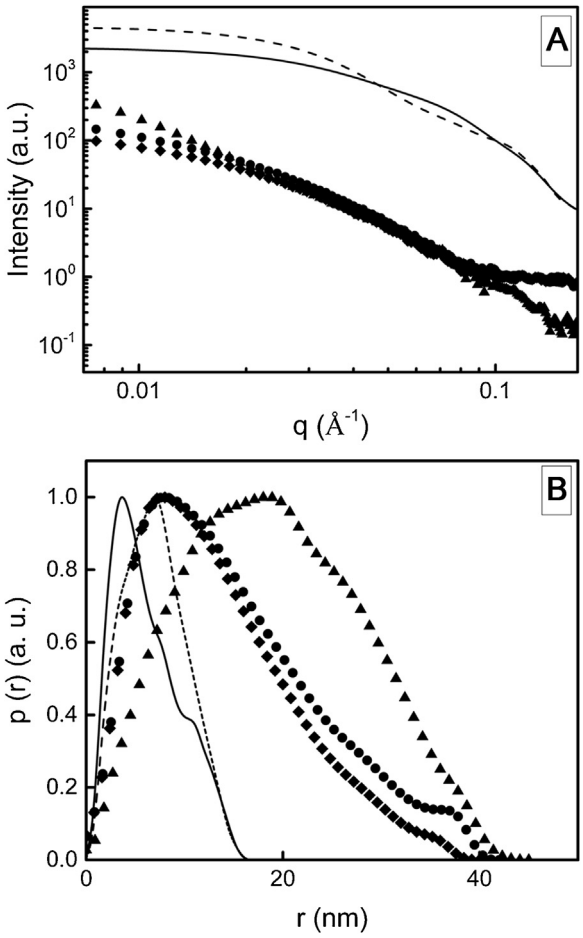

Fig. 6. (A) SAXS measurements of NKA in SDS free solution (▲), with 160:1 (●) and 320:1 (♦) SDS/Protein molar ratio, protein concentration was 0.46 mg mL^{-1} and samples were filtered using a 100 nm-pore prior to measurements. Theoretical SAXS curves of monomer (---) and dimer (—) (PDB: 3WGV). The theoretical curves are displaced for clarity. (B) Pair distance distribution function from the NKA without SDS (▲), with 160:1 (●) and 320:1 (♦) SDS/Protein molar ratio, and the theoretical SAXS curve obtained for monomer (---) and dimer (—) (PDB: 3WGV).

populations, including higher-order oligomers and aggregates, when the protein is devoid of its natural microenvinronment [30,31].

3.4. Detergent effects on protein oligomerization

In order to better investigate the protein oligomerization dependence on $C_{12}E_8$:NKA molar ratio, DLS measurements were also employed. The NKA was solubilized using 1 mg of $C_{12}E_8$ to 1 mg of protein. However, the solubilized NKA sample was thus eluted with a buffer containing 0.005 mg mL^{-1} of $C_{12}E_8$. The addition of excess detergent to the eluted sample, with final (detergent/protein) molar ratio ranging from 4 to 2100, considering 0.005 mg mL^{-1} as the basal detergent concentration, decreased the average size of the scattering particles by almost four-folds (Fig. 5A). Thus, detergent may induce the dissociation of the higher oligomeric species, preventing NKA aggregation. These results agree with those reported in Refs. [56] and [64], where changes in the NKA oligomeric structures purified from dog kidney was observed. In these articles, the authors showed that, with an increase in $C_{12}E_8$ concentration, the molar mass of the enzyme decreased, indicating that the oligomeric state is dependent on the enzyme's ambience. Moreover, it is known that huge amounts of $C_{12}E_8$ can induce the separation of α and β subunits followed by the formation of α_4 aggregates as demonstrated by Barbosa et al. [34]. In which, when the range of detergent/protein molar ratio varied between 1600:1–16,000:1, with the protein concentration as 2 mg mL^{-1}, the enzymatic activity decreased to 10% [34].

On the other hand, the detergent can form micelles in solution when it is above the CMC (0.053 mg mL^{-1}), which has a size of 7 nm (determined by DLS), and this can contribute to the average size of the particles.

At higher concentrations of the non-ionic detergent, the process of aggregation is much slower, although the enzymatic activity decreases faster. According to Ref. [56] this occurs due to delipidation, as associated lipids are essential to keep the native structure of the enzyme. Of note, the increase of $C_{12}E_8$ amount to avoid protein aggregation is not rewarding, since its activity is almost null for higher detergent quantity (Fig. 5A).

The influence of an anionic detergent was also investigated here, since it is well known that such detergents can promote dissociation of multimeric proteins by the interplay of electrostatic and hydrophobic forces [65–67]. Accordingly, we added the negatively charged SDS surfactant to the $C_{12}E_8$-solubilized NKA as a trial to obtain a homogeneous sample formed by monomers (αβ) and/or dimers $(\alpha\beta)_2$. SAXS technique was then employed to observe changes in the $C_{12}E_8$-solubilized NKA radius of gyration (R_g) (Fig. 5B) and maximum dimension (D_{max}) obtained from the distance distribution function p(r) analysis (Fig. 6). For compari-

son purposes, SAXS curves of $(\alpha\beta)$ and $(\alpha\beta)_2$ calculated from the crystallographic structures (Table 1), and the corresponding p(r) functions, are displayed in Fig. 6. Of note, both Hydropro software and p(r) analysis using 3WGV PDB file resulted in similar values of D_{max}.

In the absence of SDS, R_g and D_{max} values are three times greater than those expected for the dimer species (Figs. 5B and 6B). Therefore, enzyme oligomers/aggregates are present in the concentrated NKA sample, which is in good agreement with the analysis of absorption (turbidity), DLS and AUC. The addition of SDS causes a reduction of 27% and 33% in R_g values for the samples containing 160:1 and 320:1 SDS/NKA molar ratio, respectively (Fig. 5B). Such findings suggest that SDS interacts with NKA higher-order oligomers/aggregates promoting their dissociation. Moreover, even after increasing the molar ratio to 320:1 SDS/Protein, the R_g and D_{max} are ~2 times the theoretical values for dimer (R_g and D_{max} are 5.4 and 16 nm, respectively), indicating that even though SDS is capable of dissociating the oligomers/aggregates, the dimeric state of NKA is not reached.

On the other hand, molar ratios higher than 150:1 SDS/Protein reduce significantly the NKA activity to 10% of the basal level (Fig. 5B). As we showed previously, the major contribution to the enzymatic activity is due to the oligomers that have hydrodynamic radius smaller than 220 nm. Therefore, one can suggest that the surfactant interacts with the small enzyme forms [16,59,61] and inhibits the catalytic site and/or promotes conformational changes that lead to protein denaturation [66,68,69].

SAXS measurements combined with enzymatic activity assay hereby demonstrate that the addition of anionic detergent into the solution of $C_{12}E_8$-solubilized and purified NKA is not instructive, since it can interact with all oligomers and aggregates (big and small) resulting in a substantial decrease of the enzymatic activity.

4. Conclusion

We have shown that the $C_{12}E_8$-solubilized and purified NKA in solution is composed of an equilibrium of oligomers and aggregates. However, part of the aggregates which do not have activity can be removed by simple filtration. The residual population in solution is an equilibrium of oligomers, the monomer and tetramer being the main components as revealed by AUC measurements. However, the equilibrium can be altered by varying the protein and detergent concentrations. Besides, after the filtration, new oligomers/aggregates are formed over time. The increase in the $C_{12}E_8$ detergent concentration avoided the re-aggregation process, nonetheless the protein function is lost, probably because of the separation of the α and β subunits and/or modification in structure responsible for its activity. Similar effect was demonstrated when SDS was added to NKA. Although, it is still unclear which is the functional unit of NKA *in vivo*, it is well known that oligomerization happens in natural membranes and cannot be ruled out that this behavior could be a natural process involved in metabolic regulation of various functions in the plasma membrane of cells.

Acknowledgments

The authors thank FAPESP, CNPq, CAPES for the financial support and Pradeep Uppamoochikkal for linguistic advice. Juliana Sakamoto Yoneda and Gustavo Scanavachi received CNPq fellowship. Heitor Gobbi Sebinelli received CNPq fellowship. RI, PC, LRSB and JCB are recipients from CNPq research fellowships.

Appendix A. Supplementary data

Supplementary data associated with this article can be found, in the online version, at http://dx.doi.org/10.1016/j.ijbiomac.2016.04.058.

References

[1] I. Klodos, M. Esmann, R.L. Post, Large-scale preparation of sodium-potassium ATPase from kidney outer medulla, Kidney Int. 62 (2002) 2097–2100.
[2] P.L. Jorgensen, K.O. Hakansson, S.J. Karlish, Structure and mechanism of Na,K-ATPase: functional sites and their interactions, Annu. Rev. Physiol. 65 (2003) 817–849.
[3] J.D. Horisberger, Recent insights into the structure and mechanism of the sodium pump, Physiology (Bethesda) 19 (2004) 377–387.
[4] C. Doganli, C. Oxvig, K. Lykke-Hartmann, Zebrafish as a novel model to assess Na^+/K^+-ATPase-related neurological disorders, Neurosci. Biobehav. Rev. 37 (2013) 2774–2787.
[5] G.E. Shull, L.K. Lane, J.B. Lingrel, Amino-acid sequence of the beta-subunit of the $(Na^+ + K^+)$ATPase deduced from a cDNA, Nature 321 (1986) 429–431.
[6] P. Beguin, X. Wang, D. Firsov, A. Puoti, D. Claeys, J.D. Horisberger, K. Geering, The gamma subunit is a specific component of the Na,K-ATPase and modulates its transport function, EMBO J. 16 (1997) 4250–4260.
[7] S.P. Barwe, S. Kim, S.A. Rajasekaran, J.U. Bowie, A.K. Rajasekaran, Janus model of the Na,K-ATPase beta-subunit transmembrane domain: distinct faces mediate alpha/beta assembly and beta–beta homo-oligomerization, J. Mol. Biol. 365 (2007) 706–714.
[8] C.M. Franzin, X.M. Gong, P. Teriete, F.M. Marassi, Structures of the FXYD regulatory proteins in lipid micelles and membranes, J. Bioenerg. Biomembr. 39 (2007) 379–383.
[9] J.B. Lingrel, The physiological significance of the cardiotonic steroid/ouabain-binding site of the Na,K-ATPase, Annu. Rev. Physiol. 72 (2010) 395–412.
[10] A.Y. Bagrov, J.I. Shapiro, O.V. Fedorova, Endogenous cardiotonic steroids: physiology, pharmacology, and novel therapeutic targets, Pharmacol. Rev. 61 (2009) 9–38.
[11] L. Reinhard, H. Tidow, M.J. Clausen, P. Nissen, Na^+,K^+-ATPase as a docking station: protein–protein complexes of the Na(+),K(+)-ATPase, Cell. Mol. Life Sci. 70 (2013) 205–222.
[12] J.C. Skou, M. Esmann, The Na,K-ATPase, J. Bioenerg. Biomembr. 24 (1992) 249–261.
[13] J.P. Morth, B.P. Pedersen, M.S. Toustrup-Jensen, T.L. Sorensen, J. Petersen, J.P. Andersen, B. Vilsen, P. Nissen, Crystal structure of the sodium–potassium pump, Nature 450 (2007) 1043–1049.
[14] R. Kanai, H. Ogawa, B. Vilsen, F. Cornelius, C. Toyoshima, Crystal structure of a Na^+-bound Na^+, K^+-ATPase preceding the E1P state, Nature 502 (2013) 201–206.
[15] J.C. Skou, The influence of some cations on an adenosine triphosphatase from peripheral nerves, Biochim. Biophys. Acta 23 (1957) 394–401.
[16] K. Taniguchi, S. Kaya, K. Abe, S. Mardh, The oligomeric nature of Na/K-transport ATPase, J. Biochem. 129 (2001) 335–342.
[17] P.L. Jorgensen, J.P. Andersen, Thermoinactivation and aggregation of alpha beta units in soluble and membrane-bound (Na,K)-ATPase, Biochemistry 25 (1986) 2889–2897.
[18] R.J. Clarke, Mechanism of allosteric effects of ATP on the kinetics of P-type ATPases, Eur. Biophys. J. 39 (2009) 3–17.
[19] A. Askari, W. Huang, Na^+,K^+-ATPase: half-of-the-subunits cross-linking reactivity suggests an oligomeric structure containing a minimum of four catalytic subunits, Biochem. Biophys. Res. Commun. 93 (1980) 448–453.
[20] M. Laughery, M. Todd, J.H. Kaplan, Oligomerization of the Na,K-ATPase in cell membranes, J. Biol. Chem. 279 (2004) 36339–36348.
[21] S. Kaya, K. Abe, K. Taniguchi, M. Yazawa, T. Katoh, M. Kikumoto, K. Oiwa, Y. Hayashi, Oligomeric structure of P-type ATPases observed by single molecule detection technique, Ann. N. Y. Acad. Sci. 986 (2003) 278–280.
[22] J.C. Koster, G. Blanco, R.W. Mercer, A cytoplasmic region of the Na,K-ATPase alpha-subunit is necessary for specific alpha/alpha association, J. Biol. Chem. 270 (1995) 14332–14339.
[23] J.H. Kaplan, Biochemistry of Na,K-ATPase, Annu. Rev. Biochem. 71 (2002) 511–535.
[24] S.M. Periyasamy, W.H. Huang, A. Askari, Subunit associations of $(Na^+ + K^+)$-dependent adenosine triphosphatase. Chemical cross-linking studies, J. Biol. Chem. 258 (1983) 9878–9885.
[25] E. Tokhtaeva, R.J. Clifford, J.H. Kaplan, G. Sachs, O. Vagin, Subunit isoform selectivity in assembly of Na,K-ATPase alpha–beta heterodimers, J. Biol. Chem. 287 (2012) 26115–26125.
[26] G.G. Prive, Detergents for the stabilization and crystallization of membrane proteins, Methods 41 (2007) 388–397.
[27] J.R. Silvius, Solubilization and functional reconstitution of biomembrane components, Annu. Rev. Biophys. Biomol. Struct. 21 (1992) 323–348.
[28] C.F. Rigos, H. de Lima Santos, J.S. Yoneda, G. Montich, B. Maggio, P. Ciancaglini, Cytoplasmatic domain of Na,K-ATPase alpha-subunit is responsible for the aggregation of the enzyme in proteoliposomes, Biophys. Chem. 146 (2010) 36–41.

[29] C.F. Rigos, H. de Lima Santos, R.J. Ward, P. Ciancaglini, Lipid bilayer stabilization of the Na,K-ATPase reconstituted in DPPC/DPPE liposomes, Cell Biochem. Biophys. 44 (2006) 438–445.
[30] H. de Lima Santos, M.L. Lopes, B. Maggio, P. Ciancaglini, Na,K-ATPase reconstituted in liposomes: effects of lipid composition on hydrolytic activity and enzyme orientation, Colloids Surf. B Biointerfaces 41 (2005) 239–248.
[31] J.S. Yoneda, C.F. Rigos, T.F. de Lourenco, H.G. Sebinelli, P. Ciancaglini, Na,K-ATPase reconstituted in ternary liposome: the presence of cholesterol affects protein activity and thermal stability, Arch. Biochem. Biophys. 564 (2014) 136–141.
[32] J.S. Yoneda, C.F. Rigos, P. Ciancaglini, Addition of subunit gamma, K^+ ions, and lipid restores the thermal stability of solubilized Na,K-ATPase, Arch. Biochem. Biophys. 530 (2013) 93–100.
[33] C.F. Rigos, T.M. Nobre, M.E. Zaniquelli, R.J. Ward, P. Ciancaglini, The association of Na,K-ATPase subunits studied by circular dichroism, surface tension and dilatational elasticity, J. Colloid Interface Sci. 325 (2008) 478–484.
[34] L.R. Barbosa, C.F. Rigos, J.S. Yoneda, R. Itri, P. Ciancaglini, Unraveling the Na,K-ATPase alpha(4) subunit assembling induced by large amounts of $C_{12}E_8$ by means of small-angle X-ray scattering, J. Phys. Chem. B 114 (2010) 11371–11376.
[35] H.L. Santos, R.P. Lamas, P. Ciancaglini, Solubilization of Na,K-ATPase from rabbit kidney outer medulla using only $C_{12}E_8$, Braz. J. Med. Biol. Res. 35 (2002) 277–288.
[36] D.W. Martin, J. Marecek, S. Scarlata, J.R. Sachs, Alphabeta protomers of Na^+,K^+-ATPase from microsomes of duck salt gland are mostly monomeric: formation of higher oligomers does not modify molecular activity, Proc. Natl. Acad. Sci. U. S. A. 97 (2000) 3195–3200.
[37] J.R. Brotherus, J.V. Moller, P.L. Jorgensen, Soluble and active renal Na,K-ATPase with maximum protein molecular mass 170,000 ± 9000 Da; formation of larger units by secondary aggregation, Biochem. Biophys. Res. Commun. 100 (1981) 146–154.
[38] J.K. Heinonen, R.J. Lahti, A new and convenient colorimetric determination of inorganic orthophosphate and its application to the assay of inorganic pyrophosphatase, Anal. Biochem. 113 (1981) 313–317.
[39] B.J. Berne, R. Pecora, Dynamic Light Scattering: with Applications to Chemistry, Biology, and Physics, Wiley, New York, 1976.
[40] P. Schuck, M.A. Perugini, N.R. Gonzales, G.J. Howlett, D. Schubert, Size-distribution analysis of proteins by analytical ultracentrifugation: strategies and application to model systems, Biophys. J. 82 (2002) 1096–1111.
[41] J.C. Borges, C.H. Ramos, Analysis of molecular targets of *Mycobacterium tuberculosis* by analytical ultracentrifugation, Curr. Med. Chem. 18 (2011) 1276–1285.
[42] J. Garcia De La Torre, M.L. Huertas, B. Carrasco, Calculation of hydrodynamic properties of globular proteins from their atomic-level structure, Biophys. J. 78 (2000) 719–730.
[43] C.B. Coulter, F.M. Stone, E.A. Kabat, The structure of the ultraviolet absorption spectra of certain proteins and amino acids, J. Gen. Physiol. 19 (1936) 739–752.
[44] G.R. Grimsley, N.C. Pace, Spectrophotometric determination of protein concentration, in: J.E. Coligan, B.M. Dunn, D.W. Speicher, P.T. Wingfield (Eds.), Current protocols in protein science, John Wiley & Sons, Inc., Hoboken, N.J, 2003.
[45] S.J. Leach, H.A. Scheraga, Effect of light scattering on ultraviolet difference spectra, J. Am. Chem. Soc. 82 (1960) 4790–4792.
[46] D.B. Wetlaufer, J.T. Edsall, B.R. Hollingworth, Ultraviolet difference spectra of tyrosine groups in proteins and amino acids, J. Biol. Chem. 233 (1958) 1421–1428.
[47] A. Guinier, G. Fournet, Small-Angle Scattering of X-rays, Wiley, New York, 1955.
[48] M.G. Ortore, F. Spinozzi, P. Mariani, A. Paciaroni, L.R.S. Barbosa, H. Amenitsch, M. Steinhart, J. Ollivier, D. Russo, Combining structure and dynamics: non-denaturing high-pressure effect on lysozyme in solution, J. R. Soc. Interface 6 (2009) S619–S634.
[49] O. Glatter, O. Kratky, Small Angle X-ray Scattering, Academic Press, London, New York, 1982.
[50] L.R.S. Barbosa, F. Spinozzi, P. Mariani, R. Itri, Small-angle X-ray scattering applied to proteins in solution, in: J.M. Ruso, A. Piñeiro (Eds.), Proteins in Solution and at Interfaces, John Wiley & Sons, Inc., 2013, pp. 49–72.
[51] A. Bergmann, G. Fritz, O. Glatter, Solving the generalized indirect Fourier transformation (GIFT) by Boltzmann simplex simulated annealing (BSSA), J. Appl. Crystallogr. 33 (2000) 1212–1216.
[52] W.S. Craig, Monomer of sodium and potassium-ion activated adenosine-triphosphatase displays complete enzymatic function, Biochemistry 21 (1982) 5707–5717.
[53] J.R. Brotherus, L. Jacobsen, P.L. Jorgensen, Soluble and enzymatically stable ($Na^+ + K^+$)-Atpase from mammalian kidney consisting predominantly of protomer alpha-beta-units—preparation assay and reconstitution of active Na^+,K^+ transport, Biochim. Biophys. Acta 731 (1983) 290–303.
[54] T. Nakao, T. Ohno, M. Nakao, G. Maeki, S. Tsukita, H. Ishikawa, Monomeric and trimeric structures of active Na,K-ATPase in $C_{12}E_8$ solution, Biochem. Biophys. Res. Commun. 113 (1983) 361–367.
[55] Y. Hayashi, T. Takagi, S. Maezawa, H. Matsui, Molecular weights of alpha beta-protomeric and oligomeric units of soluble (Na^+,K^+)-ATPase determined by low-angle laser light scattering after high-performance gel chromatography, Biochim. Biophys. Acta 748 (1983) 153–167.
[56] M. Esmann, The distribution of $C_{12}E_8$-solubilized oligomers of the ($Na^+ + K^+$)-Atpase, Biochim. Biophys. Acta 787 (1984) 81–89.
[57] K. Mimura, Y. Tahara, N. Shinji, E. Tokuda, H. Takenaka, Y. Hayashi, Isolation of stable (alpha beta)(4)-tetraprotomer from Na^+/K^+-ATPase solubilized in the presence of short-chain fatty acids, Biochemistry 47 (2008) 6039–6051.
[58] C.N. Pace, F. Vajdos, L. Fee, G. Grimsley, T. Gray, How to measure and predict the molar absorption-coefficient of a protein, Protein Sci. 4 (1995) 2411–2423.
[59] G. Blanco, Na,K-ATPase subunit heterogeneity as a mechanism for tissue-specific ion regulation, Semin. Nephrol. 25 (2005) 292–303.
[60] R.J. Clarke, D.J. Kane, Two gears of pumping by the sodium pump, Biophys. J. 93 (2007) 4187–4196.
[61] C. Donnet, E. Arystarkhova, K.J. Sweadner, Thermal denaturation of the Na,K-ATPase provides evidence for alpha–alpha oligomeric interaction and gamma subunit association with the C-terminal domain, J. Biol. Chem. 276 (2001) 7357–7365.
[62] A.V. Ivanov, M.E. Gable, A. Askari, Interaction of SDS with Na^+/K^+-ATPase—SDS-solubilized enzyme retains partial structure and function, J. Biol. Chem. 279 (2004) 29832–29840.
[63] E. Tokhtaeva, R.J. Clifford, J.H. Kaplan, G. Sachs, O. Vagin, Subunit isoform selectivity in assembly of Na,K-ATPase alpha-beta heterodimers, J. Biol. Chem. 287 (2012) 26115–26125.
[64] K. Mimura, H. Matsui, T. Takagi, Y. Hayashi, Change in oligomeric structure of solubilized Na^+/K^+-ATPase induced by octaethylene glycol dodecyl ether, phosphatidylserine and ATP, Biochim. Biophys. Acta 1145 (1993) 63–74.
[65] P.P. Mishra, J. Bhatnagar, A. Datta, The interplay of hydrophobic and electrostatic effects in the surfactant-induced aggregation/deaggregation of chlorin p(6), J. Phys. Chem. B 109 (2005) 24225–24230.
[66] B.R.S. Chandra, V. Prakash, M.S.N. Rao, Association dissociation of glycinin in urea, guanidine-hydrochloride and sodium dodecyl-sulfate solutions, J. Biosci. 9 (1985) 177–184.
[67] S. Chatterjee, T.K. Mukherjee, Size-dependent differential interaction of allylamine-capped silicon quantum dots with surfactant assemblies studied using photoluminescence spectroscopy and imaging technique, J. Phys. Chem. C 117 (2013) 10799–10808.
[68] K.S. Rao, V. Prakash, Interaction of sodium dodecyl sulfate with multi-subunit proteins. A case study with carmin, J. Biol. Chem. 268 (1993) 14769–14775.
[69] D. Otzen, Protein-surfactant interactions: a tale of many states, Biochim. Biophys. Acta 1814 (2011) 562–591.